Self-Organized Hybrid Silica with Long-Range Ordered Lamellar Structure

Joël J. E. Moreau,*,† Luc Vellutini,† Michel Wong Chi Man,† Catherine Bied,† Jean-Louis Bantignies,‡ Philippe Dieudonné,‡ and Jean-Louis Sauvajol‡

Hétérochimie Moléculaire et Macromoléculaire UMR 5076, Ecole Nationale Supérieure de Chimie Montpellier, 8 rue de l'Ecole Normale 34296 Montpellier Cedex 05, France
Groupe de Dynamique des Phases Condensées UMR 5581, Université Montpellier II Place Eugène Bataillon 34095 Montpellier Cedex 05, France

Received April 20, 2001
Revised Manuscript Received July 4, 2001

Sol−gel chemistry allowed the emergence of the so-called hybrid materials,[1] and the synthesis of organopolysilsesquioxanes having a well-defined three-dimensional network owing to the presence of covalent bonds between organic and inorganic fragments.[2−7] A step beyond the synthesis of new hybrid materials, with unique properties resulting from mixing organic and inorganic at the molecular level, consists of the controlled synthesis of organized materials. The creation of hybrids with well-ordered mesopore structure[8] was recently obtained by the use of external organic surfactant templates as it was first reported in the synthesis of silica mesophases.[9] The surfactant control of phase was extended to amphiphilic molecules with a covalent bond between the silicate and the surfactant tail and led to organic−inorganic layered materials.[10]

Scheme 1. Synthesis of Bis-urea Silylated Precursor **1** and Lamellar Hybrid **L**

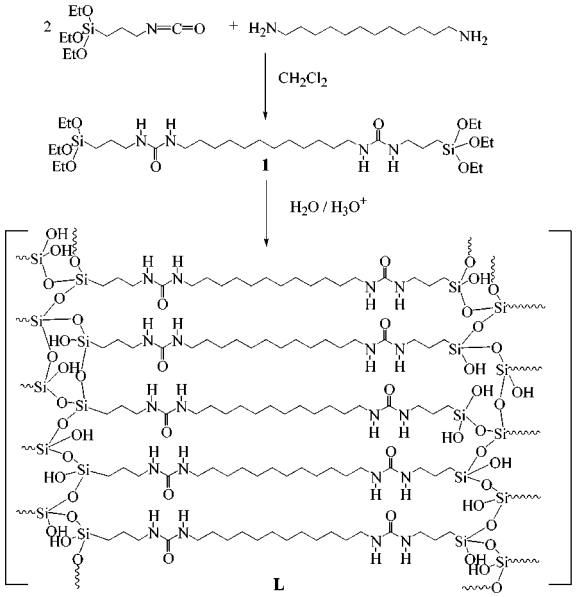

Hybrids have large potentialities since the organic component can itself exhibit diverse self-assembly properties and may direct the formation of the three-dimensional hybrid network in a self-organization process. Weak interactions between precursor molecules during the hydrolysis and condensation of $(RO)_3Si\text{-}R'\text{-}Si(OR)_3$ has been shown to influence the kinetic parameters of the gelation and to modify the texture of the resulting amorphous bridged silsesquioxanes.[6] Evidence for some anisotropic organization due to the presence of rigid aromatic segments was obtained upon examination of the birefringence properties of synthetic silsesquioxane materials.[11] Also, we recently showed that the hydrolysis of chiral units, capable of association by H-bond, allowed the creation of right and left-handed helical hybrid silica fibers, according to the (*R*,*R*) or (*S*,*S*) configuration of the 1,2-diureido-cyclohexane unit.[12] However, these hybrid materials were amorphous, and no ordered structures were reported. Here we report the first synthesis of self-organized hybrid silica with a medium long-range ordered lamellar structure. We explored the use of strong supramolecular interactions combining the association properties of urea groups by H-bond and those of long hydrocarbon chains which result from their hydrophobic properties.

A α,ω-bis-silylated molecule capable of auto-association, **1**, was readily obtained (Scheme 1) upon reaction of 1,12-diaminododecane with γ-isocyanatopropyltriethoxysilane in CH_2Cl_2. **1** was soluble in THF, EtOH, and $CHCl_3$ and formed an organogel in toluene at ca. 10 $g{\cdot}L^{-1}$, as observed for related bis-urea-based molecules.[13] Evidence for intermolecular association of the urea groups in **1** was obtained upon examination of the FTIR spectrum. Whereas diluted $CHCl_3$ solutions of **1** showed vibrations of free urea groups:[14] $\nu_{N-H} = 3445$, $\nu_{C=O}$ (amide I) = 1654 and δ_{N-H} (amide II) = 1538 cm^{-1}, in the organogel, **1** only showed H-bonded urea groups:[14] $\nu_{N-H} = 3320$, $\nu_{C=O}$ (amide I) = 1619 cm^{-1}, and δ_{N-H} (amide II) = 1576 cm^{-1}.

† Ecole Nationale Supérieure de Chimie Montpellier.
‡ Université Montpellier II.

(1) (a) Sanchez, C.; Ribot, F. *New J. Chem.* **1994**, *18*, 1007−1047. (b) Laine, R. M.; Sanchez, C.; Brinker, C. J.; Giannelis, E.; Eds. *Organic/Inorganic Hybrid Materials, MRS Symp. Vol. 519*, **1998**. (c) Klein, R. M.; Deguire, M.; Lorraine, F.; Mark, J.; Eds. *Organic/Inorganic Hybrid Materials II, MRS Symp. Vol*. 576, **1999**. (d) Laine, R. M.; Sanchez, C.; Brinker, C. J., Eds. *Organic/Inorganic Hybrid Materials III*; Materials Research Society symposium proceedings; Materials Research Society: Warrendale, PA, 2000; Vol. 628.

(2) (a) Shea, K. J.; Loy. D. A.; Webster, O. W. *Chem. Mater.* **1989**, *1*, 512−513. (b) Shea, K. J.; Loy. D. A.; Webster, O. W. *J. Am. Chem. Soc.* **1992**, *114*, 6700−6710.

(3) Corriu, R. J. P.; Moreau, J. J. E.; Thépot P.; Wong Chi Man M. *Chem. Mater*. **1992**, *4*, 1217−1224.

(4) Baney, R. H.; Itoh, M.; Sakakibara, A.; Suzuki, T. *Chem. Rev.* **1995**, *95*, 1409−1430.

(5) Loy, D. A.; Shea, K. J. *Chem. Rev.* **1995**, *95*, 1431−1442.

(6) (a) Corriu, R. J. P.; Leclercq, D. *Angew. Chem., Int. Ed. Engl.* **1996**, *35*, 1420−1436. (b) Corriu, R. J. P. *Angew. Chem., Int. Ed.* **2000**, *39*, 1376−1398.

(7) Moreau, J. J. E.; Wong Chi Man M. *Coord. Chem. Rev.* **1998**, *178*−*180*, 1073−1084.

(8) (a) Inagaki, S.; Guan, S.; Fukushima, Y.; Ohsuna, T.; Terasaki, O. *J. Am. Chem. Soc.* **1999**, *121*, 9611−9614. (b) Melde, B. J.; Holland, B. T.; Blanford, C. F.; Stein, A. *Chem. Mater.* **2000**, *11*, 3302−3308. (c) Asefa, T.; MacLachlan, M. J.; Coobs, N.; Ozin, G. A. *Nature* **1999**, *402*, 867−871. (d) MacLachlan, M. J.; Asefa, T.; Ozin, G. A. *Chem. Eur. J.* **2000**, *6*, 2507−2511. (e) Guan, S.; Inagaki, S., Y.; Ohsuna, T.; Terasaki, O. *J. Am. Chem. Soc.* **2000**, *122*, 5660−5661. (f) Sayari, A.; Hamoudi, S.; Yang, Y.; Moudrakovski, I. L.; Ripmeester, J. R. *Chem. Mater.* **2000**, *12*, 3857−3863. (g) Stein, A.; Melde, B. T.; Schroden, R. C. *Adv. Mater.* **2000**, *12*, 1403−1419. (h) Lu, Y.; Fan, H.; Doke, N.; Loy, D. A.; Assink, R. A.; LaVan, D. A.; Brinker, C. J. *J. Am. Chem. Soc.* **2000**, *122*, 5258−5261.

(9) (a) Kresge, C. T.; Leonowicz, M. E.; Roth, W. J.; Vartuli, J. C.; Beck, J. S. *Nature* **1992**, *359*, 710−712. (b) Qisheng Huo; Margolese, D. I.; Ciesla, U.; Pingyun Feng; Gier, T. E.; Sieger, P.; Leon, R.; Petroff, P. M.; Schüth, F.; Stucky, G. D. *Nature* **1994**, *368*, 317−321. (c) Mercier, L.; Pinnavaia, T. J. *Adv. Mater.* **1997**, *9*, 500−503. (d) Tanev, P. T.; Liang, Y.; Pinnavaia, T. J. *J. Am. Chem. Soc.* **1997**, *119*, 8616−8624.

(10) (a) Huo, Q. S.; Margolese, D. I.; Stucky, G. D. *Chem. Mater.* **1996**, *8*, 1147−1160. (b) Shimojima, A.; Sugahara, Y.; Kuroda, K. *Bull. Chem. Soc. Jpn.* **1997**, *70*, 2847−2853. (c) Katagiri, K.; Ariga, K.; Kikuchi, J. *Chem. Lett.* **1999**, 661−662.

(11) (a) Boury, B.; Corriu, R. J. P.; Le Strat, V.; Delord, P.; Nobili, M. *Angew. Chem., Int. Ed.* **1999**, *38*, 3172−3175. (b) Ben, F.; Boury, B.; Corriu, R. J. P.; Le Strat, V. *Chem. Mater.* **2000**, *12*, 3249−3252.

(12) Moreau, J. J. E.; Vellutini, L.; Wong Chi Man, M.; Bied, C. *J. Am. Chem. Soc.* **2001**, *123*, 1509−1510.

(13) Van Esch, J.; De Feyter, S.; Kellogg, R. M.; De Schryver, F.; Feringa, B. L. *Chem. Eur. J.* **1997**, *3*, 1238−1243.

(14) Jadzyn, J.; Stockhausen, M.; Zywucki, B. *J. Phys. Chem.* **1987**, *91*, 754−757.

10.1021/ja016053d CCC: $20.00
Published on Web 07/20/2001

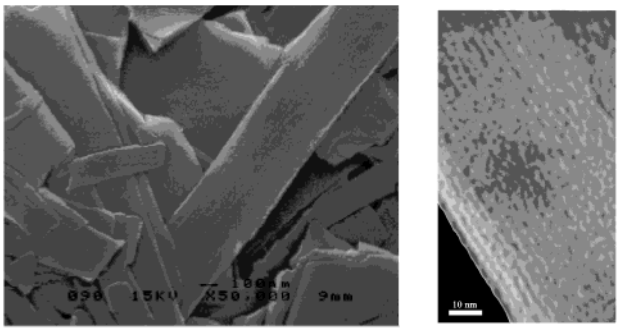

Figure 1. SEM (left) and TEM (right) images of the lamellar and well-ordered structure of hybrid **L**.

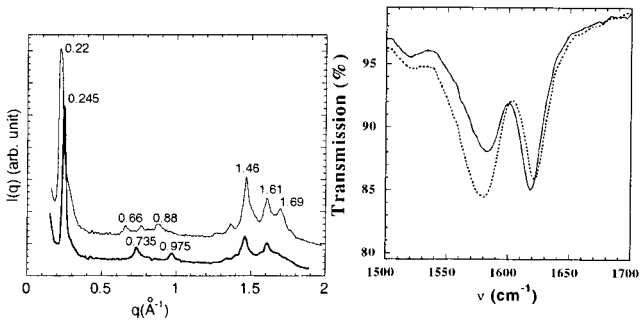

Figure 2. (a) Diffraction diagram of hybrid **L** (upper line) and **L′** (bottom line). (b) Polarized IR spectra of **L** obtained byATR: H (solid line) and V (dotted line) polarizations.

The hybrid solid **L** was then synthesized upon hydrolysis of **1** under acid catalysis (Scheme 1). In a typical synthesis, a mixture containing a molar ratio of **1**:1; H_2O:600; HCl:0.2 was vigorously stirred at 80 °C for an hour and then allowed to stand for 48 h at the same temperature. The solid which formed quantitatively was recovered by filtration and washed successively with H_2O, EtOH, and acetone. After drying (100 °C, 6 h), the solid was collected as a colorless powder.

The solid-state ^{13}C CPMAS NMR of **L** showed a peak at 160 ppm (C═O resonance) in addition to the different sp^3 carbon atoms at 43, 34, 31, 26, and 10 ppm. The ^{29}Si MAS NMR spectrum, using a HPDEC sequence, exhibited three signals at $-49(i = 0.27)$, $-58(i = 0.63)$, and $-67(i = 0.10)$ ppm, respectively assigned to $SiC(OH)_2(OSi) = (T^1)$, $SiC(OH)(OSi)_2 = (T^2)$ and $SiC(OSi)_3 = (T^3)$ substructures. It is indicative of a moderately condensed siloxane network with an average of one uncondensed OH group per silicon atom. The analytical results (C: 48,51; H: 8,74; N: 11,49; Si: 11,15%) are consistent with the above NMR results and atomic composition. No cleavage of the urea groups or Si−C bonds occurred under the synthesis conditions.

SEM images revealed that **L** has an homogeneous lamellar morphology which consists of thin plates up to 1−2 μm large, 3−5 μm long, and 50−100 nm thick (Figure 1). Interestingly, TEM images confirmed a layered structure by showing some well-ordered features with lamellar spacing.

The X-ray diffraction spectrum of the hybrid solid **L** (Figure 2a) with intense Bragg peaks indicates a material with medium long-range order. The first intense peak at 0.22 $Å^{-1}$ indicates that the observed longer characteristic distance is ∼28 Å. Peaks at 0.66 and 0.88 $Å^{-1}$ could be associated to third- and fourth-order of the peak at 0.22 $Å^{-1}$. This distance close to the length of the precursor **1** is compatible with the interlayer spacing observed on TEM images. The half width at half-maximum of this peak, ∼0.02 $Å^{-1}$, leads to a correlation length of ∼315 Å in the same order of magnitude as the plate thickness and in agreement with a long-range lamellar ordering in the plates observed in TEM in Figure 1. Other peaks at 1.46, 1.61, and 1.69 $Å^{-1}$ could be associated to in-plane ordering.

To confirm the above assignments, we synthesized under identical conditions a hybrid **L′** from a similar precursor but with a shorter C_{10} hydrocarbon chain (instead of C_{12} in **1**). **L′** exhibited NMR, IR, SEM, and TEM characteristics similar to those of **L**. It is interesting to compare the X-ray diffraction spectra of **L** and **L′** (Figure 2). Similar patterns are observed for both solids with slight differences regarding peaks at low q values. The latter shift toward higher q values: 0.245 $Å^{-1}$, 0.735 $Å^{-1}$, 0.975 $Å^{-1}$ consistently with the above assignments with a decrease in the lamellar spacing to ∼26 Å and with a reduction of the length of the hydrocarbon chain in the precursor. Also consistently, peaks in the region 1.46−1.69 $Å^{-1}$ exist at the same position for **L** and **L′** and do not depend on the interlayer spacing. For both solids **L** and **L′**, the non observation of the second-order of the lower q diffraction peak should be associated to a minimum of the structure factor at the corresponding q value.

Anisotropic orientation was also studied by FTIR upon examination of the polarization dependence of the vibration modes using "attenuated total reflection" (ATR) (Figure 2b). H polarization refers to transmission spectra obtained with the electric vector parallel to the diamond/lamella interface, V polarization refers to transmission spectra with the electric vector at 45° of the interface. Both amide I ($\nu_{C=O}$) and amide II (δ_{N-H}) modes show a polarization dependence. The modes at 1618 cm^{-1} ($\nu_{C=O}$) and 1583 cm^{-1} (δ_{N-H}) in the H polarization shift respectively to 1621 and 1579 cm^{-1} in the V polarization. $\Delta\nu$ (amide I − amide II) is equal to 35 cm^{-1} in the H polarization and 42 cm^{-1} in the V polarization. By contrast, this difference $\Delta\nu$ is equal to 120 cm^{-1} in free molecules. The strong reduction of $\Delta\nu$ in the hybrid is in perfect agreement with the presence of H-bonded urea groups.[14] The decrease of $\Delta\nu$ in H compared to V polarization could be related to a more significant contribution of the H-bond strength for modes polarized in the H polarization than those polarized in the V polarization. It is consistent with the model in Scheme 1, assuming that the pressure applied on the sample induces the orientation of the layers parallel to the ATR prism surface. Especially, the decrease of $\Delta\nu$ in H compared to V polarization supports the model of a planar H-bonded urea groups network belonging to the stacking layer.

The above observations show that the synthesis of the hybrid solid, which results from the formation of strong covalent siloxane (Si−O−Si) bonds, is controlled by weak intermolecular interactions between the organic substructures. The lamellar structure probably results from a controlled condensation reaction, owing to interactions developing between monomeric units or growing oligomers. Acid catalysis which leads to a slow and moderate condensation of the silicate units probably facilitate the ordering of the organic fragments owing to a rigidity of the siloxane network that is lower when it consists of T^2 substructures than when it contains fully condensed T^3 substructures. However, the precursor **1** did not completely dissolve in water−HCl before condensation, and the reaction is heterogeneous. Further studies are necessary to clarify the exact mechanistic pathway.

We are also currently extending this organically self-directed generation of hybrid solids. Self-organization by H-bonds is an attractive point of these materials. Hybrid solids are of great interest for a variety of applications which cover molecular recognition, advanced catalysis, transport, electronic, optoelectronic, or magnetism. In this context, the control of the structure of the material is important not only at the molecular level but also at the nanoscopic and macroscopic levels.

Acknowledgment. Support from the "Ministère de la Recherche" and from the CNRS is gratefully acknowledged.

JA016053D